# SOME EXAMPLES OF THE PREDICTION AND VALIDATION OF NEAR-FIELD DEPENDENT AIRCRAFT HF ANTENNA PARAMETERS USING NEC

J. W. R. Cox
Air Tactical Communications Division
Space & Communications Department
Defence Research Agency
Farnborough
Hampshire, UK

## ABSTRACT

Examples are presented of the application of a moment-method modelling procedure (using NEC) to calculate the near-field dependent parameters of aircraft HF antennas. The overall aim of the work from which the examples are drawn is to provide a 'recipe'; the application of which will generate predictions of parameters of interest which are both credible and sufficiently accurate for engineering purposes. A feature of the procedure is that no empirically derived information is incorporated. The examples encompass a range of generic aircraft and antenna types: both fixed and rotary wing airframes, and electric (wire) and magnetic (loop and notch) primary radiators. Particular emphasis is placed upon validation of the predictions. This is performed by direct measurement where possible, but where this is not practicable simple, but independent, calculations are performed based upon equivalent circuits. As for the moment-method procedure, these corroborative calculations do not depend upon empirical information.

## INTRODUCTION

At HF (2-30 MHz) airframes are resonant at numerous frequencies throughout the band and modelling procedures must be sufficiently sound to predict such resonances and their effect upon parameters of interest. Thus, near-fields must be calculated accurately for this general reason as well as the more particular one of predicting the actual value of parameters which depend upon the near-field (*eg* antenna reactance, coupling between antennas etc). Accurate calculation of the near-field requires good solutions for the body surface currents and this implies high sampling densities. There are, however, limitations to the sampling density which can be contemplated. The more obvious practical limitations are:

(i) time taken to construct mathematical models;
(ii) run times;
(iii) factors depending upon machine precision, basis functions, matrix size, and the possible consequences for solution stability.

For those involved in practical calculations pertinent questions therefore are:

(a) How high does the sampling density need to be for engineering purposes?
(b) How credible are the results?

The answers to these questions depend of course upon particular circumstances and requirements, but it is hoped that the following examples might be of some use in this regard.

In evolving the methods described here, it was considered important that the modelling procedure would be truly predictive: that is, it should not involve any empirically derived information. For the examples cited below, construction of the mathematical model is performed only with the aid of general arrangement drawings and (when available) photographs or models. The reason for this is that predictions of the likely performance of a proposed antenna system are usually required early in a project cycle prior to the airframe being available for measurement, or even in existence at all. Indeed if circumstances are otherwise it is sometimes better to generate the required information by other means. Thus, the same modelling procedure was used without *ad hoc* modification for each of the examples, and is as follows.

## MOMENT-METHOD MODELLING PROCEDURE

For aircraft-like (that is, non-voluminous) structures in the HF band, the solution stability problems of the magnetic field integral equation (MFIE) preclude its use unless prohibitively high sampling densities are adopted. Use of the electric field integral equation was therefore considered necessary. The aircraft surface is modelled as a wire-mesh and discretized with the aim of producing an approximately square mesh (becoming triangular when required by local topology) with a mesh side of about 0.0025 wavelength (0.3 to 0.4 m) at the bottom of the band (2 MHz). The solution code is a single precision version of NEC3(1) with modifications to facilitate running on a Cray 1 machine. The sampling density was made one match point per mesh side. The radii of the mesh wires are such that the resulting surface area of each wire when notionally 'unwrapped' is the same as that of the surface that it replaces. In effect this represents an attempt to satisfy (approximately) the MFIE, the first term of which represents Ampere's law at a portion of a perfectly conducting closed surface. That is, the magnetic field boundary conditions are approximately satisfied, in addition to the electric field boundary conditions that are imposed at the match points.

## VALIDATION OF MOMENT-METHOD PREDICTIONS

A means of quantitatively assessing the validity of moment-method calculations for small-scale problems is to examine the convergence of solution. That is, the discretization is successively refined and the predicted result of some parameter of interest examined after each calculation. The anticipation is that the result at each stage will converge asymptotically to the 'true' value. This is not a practical proposition for large scale problems of the type considered here: the constraints of successively longer periods for model construction and run times preclude this. Thus, experimental and/or independent theoretical means must be sought for validation.

A major problem in assessing the credibility of predictions concerning aircraft HF antennas by experimental means is the frequently encountered impracticability of measuring some parameters of engineering interest. An obvious example is radiation resistance: at the low frequency end of the band this is, in the vast majority of cases, much smaller than the airframe loss resistance and cannot be determined by a measurement made at the antenna terminals. It is clearly not a practical proposition to measure the total radiated power in order to deduce the radiation resistance. In addition, to measure those parameters which could be determined experimentally is often prohibitively expensive because of engineering work which must first be performed upon the aircraft. This is particularly true of smaller aircraft where antenna terminals are often located at positions which are inaccessible when the aircraft is in flight. Thus, independent supporting evidence against which the credibility of predictions can be assessed is usually meagre and so, whatever direct or circumstantial information and physical insight which is available must be exploited: these difficulties have been considered elsewhere (2).

In the examples considered below only in one case was direct (that is, in flight) experimental evidence obtainable for corroboration of near-field parameters. This was because the subject was a medium-size passenger aircraft and the terminals were easily accessible from within the fuselage. In another example, terminal measurements were only practicable for the aircraft located on the ground; this involves additional effects and complications which are not easy to quantify. In another case indirect evidence is sought from radiation patterns: predicted patterns were compared with those derived from measurements made upon a physical scale model, and upon a real aircraft in flight. Although a far-field dependent property, radiation patterns show evidence of airframe resonances and therefore give an indication of the accuracy with which near-fields are calculated.

Where experimental corroboration is not practicable, equivalent circuit models are derived to assess the credibility of the moment-method calculations. The circuit parameters for these models are derived in a logical manner and not simply adjusted to fit the moment method predictions. These circuits, however, involve the application of insight in their construction, considerable simplification to maintain tractability (and therefore the introduction of an element of subjectivity), and can only be convincingly produced for certain antenna types and configurations. It is of course unreasonable to expect good agreement between the moment-method calculations and those derived from an equivalent circuit. In fact the circuit model can really serve to give only an indication as to whether the moment-method calculations are, or are not, credible. One reason for this is that in those cases where the construction of a simple equivalent circuit is possible, the antennas are located near, but not precisely at, the electrical centre of the fuselage. The readily obtainable usable expressions or tabulated values for Z, the impedance of the dipole representing the fuselage (see below) are, however, derived for centre excitation. Fortuitously for the two examples (2,9) in which equivalent circuits are constructed the antennas are located at approximately 40% along the electrical length of the fuselage. In addition, in both of these cases the resulting circuit component values are such that Z does not exercise a dominating influence on the final result. Thus, notwithstanding these shortcomings, it is expected that, when applicable, quantitative agreement between the moment-method calculation and the equivalent circuit would be to better than an order of magnitude. By this means therefore, a relatively crude, but independent, piece of theoretical supporting evidence can be produced.

The calculations (that is, moment-method and equivalent circuit) share a common deficiency: neither incorporate any allowance for the effects of non-zero impedance of the mechanical joints which unavoidably exist on real aircraft. As far as HF aircraft antenna performance in general is concerned these extraneous impedances are a perennial source of difficulty. This is because throughout much of the band most aircraft are not electrically large. This inevitably implies that radiation resistance and, in practice radiation efficiency, tends to be relatively small: estimated values of below 0.1% are not uncommon at the bottom of the band. Not only are joint impedances unknown (and, for practical purposes, unknowable) but they vary between nominally identical aircraft and, in the mechanically harsh environment experienced by aircraft, change over time. Thus the assumption of perfect conductivity for calculations is practically inevitable as far as such joints are concerned. Since the extraneous resistance due to joints is usually dominant over much of the band (experience indicates that measured terminal resistance is much greater than that calculated on the assumption of no joints at all), there is little to be gained by assuming other than a perfectly conducting airframe. That is, the calculated terminal resistance is the radiation resistance here.

In one of the airframe examples there are significant portions of the aircraft skin made from non-metallic material. It was noted, however, that large areas of metal existed immediately behind the skin. It was therefore considered realistic, at least at HF, to neglect the skin and treat the surface as perfectly conducting and electrically bonded to the rest of the airframe. It is expected that such bonding of internal metal structures will be arranged to afford protection against lightning strike.

**Example 1:** Terminal reactance of a medium-size passenger aircraft.

Three 'long-wire' antennas are fitted to the aircraft: the arrangement is shown in Fig 1. The model comprises 7736 segments and this is the number of unknown currents. This antenna type and configuration presents potential sources of computational difficulty. These are considered more fully elsewhere (3) but briefly they are connected with:

(1) The very close electrical proximity of the match points in the region of the antenna feed point and near the antenna anchoring point at the tail fin. The match point separation distances are around 1/3000 and 1/1500 of a wavelength respectively for these two regions.

(2) The problem of distribution of electric charge between wires of disparate radii at junctions. An incidental advantage of adopting a very fine mesh is that the radii of the wires simulating the fuselage become smaller. In addition, the ratio of the radius of the wires simulating the fuselage to that of the antenna wire falls as the mesh is made finer. For the junction treatment (based upon a study of the tapered antenna by Wu and King (Ref 4)) used in NEC, when the wires become electrically very thin the linear charge density at each of the wires at a junction is the same and does not depend strongly on the wire radii. Thus for finer meshes it is anticipated that the solutions become less dependent upon the arrangement made for dealing with junctions. Even with the high sampling densities used here, however, the ratio referred to above is still about 19. The concern is that if unrealistic charge distributions at the base (that is, the terminals) of a wire antenna are computed, these may be expected to have a significant effect upon the calculated terminal impedance.

Comparison between prediction and measurement for the terminal reactance is depicted in Fig 2 with allowance made for the presence of the lightning spark gap and other measured stray reactances present in the real installation (in effect a 'front-end' network to the actual antenna terminals) but which cannot easily be incorporated directly in a moment-method model (see Ref 3). It is seen that the resonances are predicted to within about 10% of the measured values.

**Example 2:** Calculation of maximum mutual coupling between two HF loop antennas mounted upon a helicopter at the bottom of the HF band.

The arrangement is depicted in Fig 3. There are 2250 segments in the model. The maximum mutual coupling is a function of the Y parameters of the configuration (see Ref 2) and its estimation is sensitive to the accuracy with which these parameters are calculated. Validation of the moment-method calculations was attempted by the derivation of an equivalent circuit. Below the first airframe resonance physical considerations suggest that the airframe resembles an electric dipole which is shunt fed by the driven loop antenna. Thus the dominating elementary radiating modes would be expected to be as indicated in Fig 4. In this spectral region, and for this type of antenna, it is expected that the coupling mechanism between the driven antenna and the non-driven antenna is primarily magnetic. That is the driven antenna excites the other principally by transformer action. The equivalent circuit for the arrangement is illustrated in Fig 5. An approximate estimate of the mutual inductance, $M$ , between the two tail-cone mounted antennas, was made by treating the arrangement as a DC quasi-two-dimensional problem and performing a moment-method calculation. An elementary calculation of the remaining inductances was made using the method of images in conjunction with a procedure which has been termed by Roters (5) as 'estimating the permeances of probable flux paths'. The radiation resistance, $r_1$, of the loop is estimated using the well-known expression for an electrically small magnetic dipole with allowance made for the fact that it is mounted on a conducting surface. A more detailed account of the derivation of the equivalent circuit is given in Ref 2. The impedance, $Z$ , of the dipole representing the fuselage was estimated using the following analytical expression (6).

$$Z = R(k\ell) - j[120(\ln(\ell/a) - 1)\cot(k\ell) - X(k\ell)] , \tag{1}$$

where $\ell$ is the half length of the dipole, $a$ its radius, and $k$ the free space wave number of the excitation, the functions $R(k\ell)$ and $X(k\ell)$ are tabulated in Ref (6). This expression is not, however, valid at frequencies higher than the first resonance.

Comparison of the maximum mutual coupling calculated by the two methods is shown in Fig 6. The error bars in Fig 6 are a consequence of the uncertainty in assigning a figure to the equivalent radius of the dipole representing the fuselage, and indicate the extreme possible values.

An indicator of solution quality can also be made by examining compliance with reciprocity. This is shown in the following table.

| Frequency (MHz) | Current at antenna 2 terminals while short-circuited and antenna 1 driven with excitation | Current at antenna 1 terminals while short-circuited with antenna 2 driven with excitation |
|---|---|---|
| | of 1V (A) | of 1V (A) |
| 2 | $-0.72 \times 10^{-7} + j\,0.15 \times 10^{-3}$ | $-0.85 \times 10^{-7} + j\,0.17 \times 10^{-3}$ |
| 3 | $0.59 \times 10^{-6} + j\,0.12 \times 10^{-3}$ | $0.62 \times 10^{-6} + j\,0.13 \times 10^{-3}$ |
| 4 | $0.57 \times 10^{-5} + j\,0.11 \times 10^{-3}$ | $0.61 \times 10^{-5} + j\,0.12 \times 10^{-3}$ |
| 5 | $0.42 \times 10^{-4} + j\,0.13 \times 10^{-3}$ | $0.46 \times 10^{-4} + j\,0.14 \times 10^{-3}$ |
| 6 | $0.51 \times 10^{-4} + j\,0.33 \times 10^{-4}$ | $0.73 \times 10^{-4} + j\,0.42 \times 10^{-4}$ |

**Table 1 Compliance with reciprocity**

**Example 3:** Determination of antenna impedance for a notch antenna installed on a variable geometry aircraft.

The model is constructed in such a way that it can be reconfigured as a real aircraft of this type might change its geometry. That is, alterations to the model for various positions of the moveable parts correspond exactly to the geometrical changes of the wing or taileron positions alone; there is no remeshing or any other *ad hoc* alternations made to the model (9,10). Figs 7 and 8 indicate the model with the wings in the fully forward and swept back positions. There are 3293 segments in the model. It was considered that the following factors might be a potential source of computational difficulty.

(i) The moveable surfaces clear the rest of the airframe by electrically very small distances (of the order of 1/1500 of a wavelength at 2 MHz). In addition this necessitates the use of very short segments (representing pins for mechanical pivoting) in the model which are of a similar electrical length to this figure.

(ii) The area of the notch antenna is of the order of the mesh size. In the context of running NEC on 32-bit machines, difficulties have been indicated for problems involving small loops (7). Although the work reported here was performed with single precision on 64-bit machines, it is considered that calculations should be regarded with caution particularly in view of the large and complex nature of the structures.

Validation of predictions of the terminal impedance made for the aircraft in flight was attempted by two methods. The first was to derive an equivalent circuit in a manner similar to that indicated for the previous example. The second was by measurement of terminal impedance with the aircraft on the ground.

The equivalent circuit is show in Fig 9. As indicated above, the use of equation (1) to calculate Z is limited to frequencies below the first airframe resonance. In addition to using equation (1), Z was also estimated assuming that the effect of dipole thickness on the antenna terminal impedance is not too great. This is, of course, a rather gross approximation, but it does permit values of Z to be obtained beyond the first airframe resonance using tabulated results using Wu's theory (8).

The ground measurements were performed using a vector impedance meter (VIM). Such measurements are not entirely straightforward because the effects of the cable which is required to connect the VIM to the antenna terminals must be removed from the data in order to extract the terminal impedance. This aspect is reported in more detail, along with checks of the experimental method, in Ref 10.

Comparison between the NEC calculation, the equivalent circuit model, and the ground measurements are depicted in Fig 10 for the terminal reactance. As indicated above it is not possible to extract the radiation resistance from the measured terminal resistance; hence for the former parameter, the moment-method predictions can only be compared with those of the equivalent circuit (see Fig 11). Elementary considerations suggest that the reactance should increase monotonically throughout the band and remain positive. This is observed for the calculations and measurements. It is seen that the values derived by measurement are about 36% below those of the NEC calculation over that part of the band which is approximately linear. This figure is comparable with a similar difference (26%) between measured and theoretical values (from an analytical expression) performed as a check of the measurement procedure and made on a circular loop having an area comparable to that of the notch (10).

It is expected from simple physical considerations that the longitudinal airframe resonances will occur around those frequencies at which the electrical length of the airframe is an integer multiple of half the radiation wavelength. They are approximately 7.6, 15.2 and 22.8 MHz for this example. The form of the equivalent circuit (see Fig 9) and the fact that the radiation resistance of the dipole is always significantly greater than that of the notch ($r_1$), suggests that such effects are expected to be noticeable in the NEC calculations even though resonance is a phenomenon associated with the near-field whereas radiation resistance is a far-field property. It is seen in Fig 11 that the results of the NEC calculation show disturbances which occur close to the above values of resonant frequency. Such effects re not observed for the reactance (Fig 10) because the component values are such that the shunting effect of Z is not such as to be large at any frequency in the band; not even at a series resonance. The pronounced oscillations seen in Fig 11 for the equivalent circuit model are a result of the thin wire approximation for the fuselage. Such oscillations would not be expected to be so marked in the case of a large diameter dipole such as that forming the real fuselage and it is seen in Fig 11 that they are only just perceptible on the curve for the NEC calculation. Interestingly, the two methods display a reasonable agreement at the series resonances (7.6 and 22 MHz). At such frequencies the representation of the fuselage by a thin wire would not be expected to exert a great influence to the radiation resistance estimated using the equivalent circuit.

**Example 4:** Inference of first longitudinal airframe resonant frequency from radiation patterns.

This helicopter was fitted with a loop antenna and is as depicted in Fig 12. There are 2682 segments in the model. The example is included to indicate that, as far as validation is concerned, radiation patterns can be used to indicate quality of solution even though radiation patterns depend upon the far-field. This is because, at HF, airframes are generally resonant at numerous frequencies throughout the band. For this example measurements of radiation patterns were made both using a scale physical model and with a real aircraft in flight. Details of this study along with a set of radiation patterns throughout the HF band is recorded elsewhere (11). The first airframe resonance is usually apparent in azimuthal radiation patterns for horizontal polarisation. It is characterised by a deep null in the general nose and tail directions. The nulls do not lie exactly on the nose-tail axis unless the antenna itself is also located symmetrically about this line. Greater complexity of the patterns at higher frequency resonances renders such unambiguous interpretation less likely than in the case of the first airframe resonance. This is due to the corresponding increase in the number of possible radiation modes which will, in general, be present. For the antenna orientation adopted here, the length of the probable RF current path indicates that the first longitudinal airframe resonance should be in the region of 6 MHz. Figs 13 -15 indicate a succession of such patterns as the frequency is increased through the first airframe resonance. These figures show the anticipated resonance occurs around 5.6 MHz. In passing it is noted that the patterns display the fact that the antenna is located on the left side of the aircraft. This is seen from the slightly higher levels of radiation on this side and if no experimental evidence was available would provide a simple but nevertheless useful additional indicator of the credibility of the calculations.

Examination of Figs 13-15 indicate in addition an aspect which is of some practical importance; namely that there is a level of precision in calculations beyond which there is only limited practical benefit in proceeding at least in the case of radiation pattern prediction at HF. This is due to the difficulty of making measurements reliably and repeatably with real aircraft and is in part due to the stochastic nature of the propagation conditions in this spectral region. Thus, there is some uncertainty as to what the 'correct answer' actually is.

## CONCLUSIONS

For the examples presented, the moment-method calculations seem generally consistent with such attempts at validation as could be made, and it is considered that they enhance the degree of confidence which can be placed in the prediction of near-field dependent parameters for large scale problems involving aircraft. For the aircraft HF case at least, the difficulty of quantifying the electrical properties of joints present on the airframe, and the variability of the propagation conditions, limit the precision which is, in practice, useful when calculations are required for the estimation of certain system parameters such as link budgets and for the prediction of radiation patterns.

## REFERENCES

1 Burke, G.J. and Poggio, A.J., "Numerical Electromagnetic Code – Method of Moments", NOSC Technical Document 116, Vols.1 and 2, January 1981

2 Cox, J.W.R., 1993, "Corroboration of a moment-method calculation of the maximum mutual coupling between two HF antennas mounted upon a helicopter', IEE Proc. Part H, Vol.40, No.2, April 1993, pp 113-120

3 Cox, J.W.R., "Comparison of predicted aircraft wire antenna terminal impedance (using NEC) with measurement in the HF band", Proc. 7th Int. IEE Conf. on Antennas and Propagation, York, UK, 1991, Conf. Publication No.333, pp 717-720,

4 Wu, T.T. and King, R.W.P., "The tapered antenna and its application to the Junction problem for thin wires", IEEE Trans. Antennas and Propagation, AP 24, pp 42-45, January 1976

5 Roters, H.C., "Electromagnetic devices", Wiley, New York, 1944, Chapter 5.

6 Johnson R. and Jasik, H., "Antenna Engineering Handbook", McGraw-Hill, 1984, pp 4.4-4.6

7 Burke, G.J., "Recent advances to NEC: applications and validation", AGARD Lecture Series No.165 – "Modern antenna design using computers and measurement: Application to problems of military interest", pp 3-1 to 3-25

8 King, R.W.P. and Harrison, C.W., "Antennas and waves: a modern approach", Table A.4.2, pp 753-757, The MIT Press, 1969

9 Cox, J.W.R., "Calculation of HF notch antenna terminal impedance for variable geometry aircraft", Proc. 8th Int. IEE Conf. on Antennas and Propagation, Edinburgh, UK, 1993, Conference Publication No.370,, pp 912-916

10 Cox, J.W.R., "Problems concerning the validation of moment-method models of small aircraft in the HF band", IEE Colloquium on validation and application of design tools for antennas, IEE London, June 1993, Digest No.1993/147, pp 6.1-6.8

11 Cox, J.W.R. and Vongas, G., 1991, "Calculated and measured radiation characteristics of an HF loop antenna mounted upon a helicopter", Proc. 5th Int. Conf. on HF Radio Systems and Techniques, Edinburgh, UK, 1991, Conf. Publication No.339, pp 73-78,

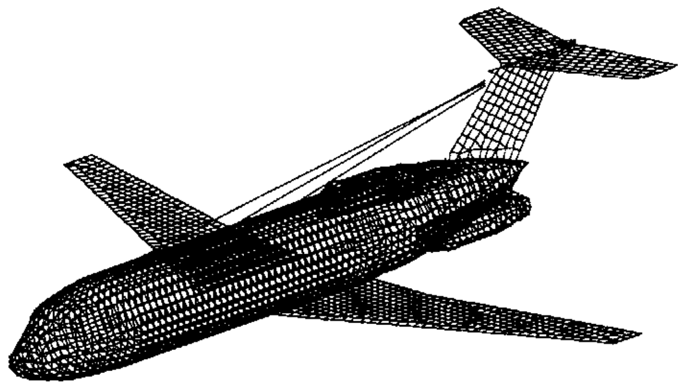

**Fig 1**

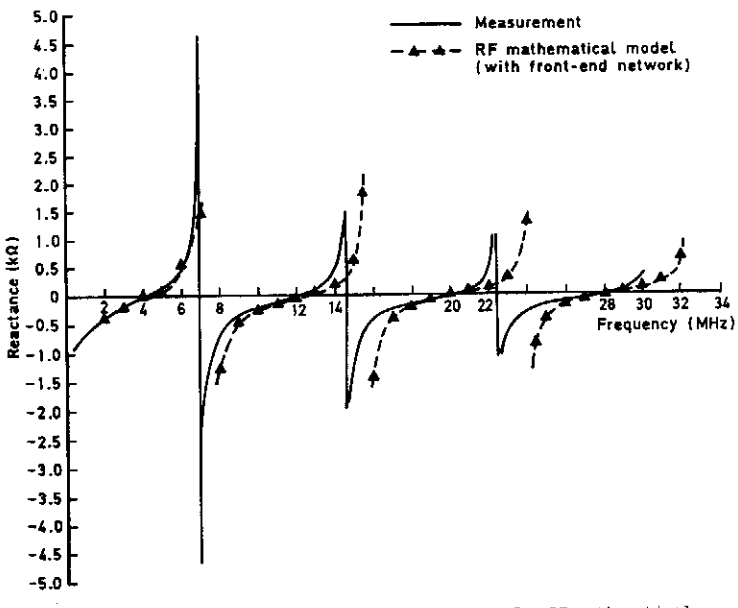


Terminal reactance versus frequency for RF mathematical model with front-end network compared with measurement

**Fig 2**

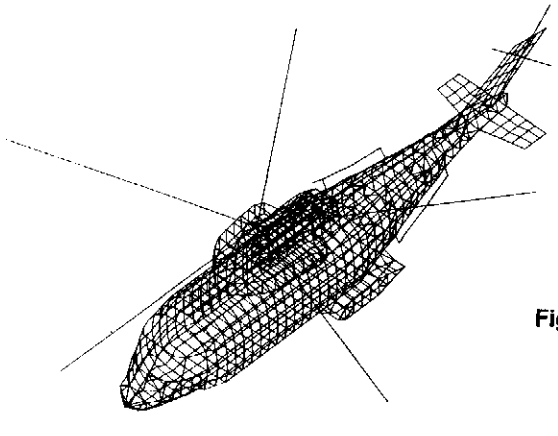

**Fig 3**

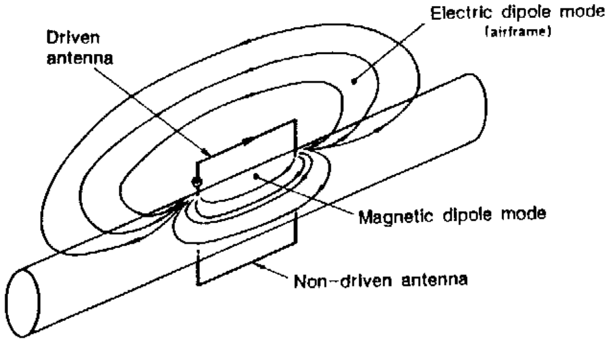


**Elementary radiating modes at frequencies below the first longitudinal airframe resonance**

**Fig 4**

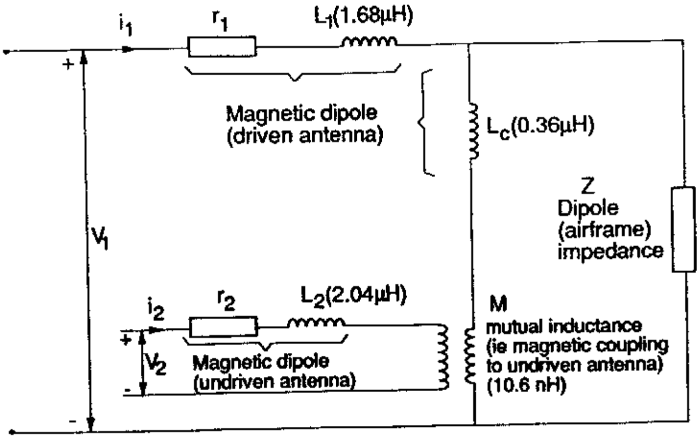


**Approximate equivalent circuit for elementary radiating modes and coupling to undriven antenna**

**Fig 5**

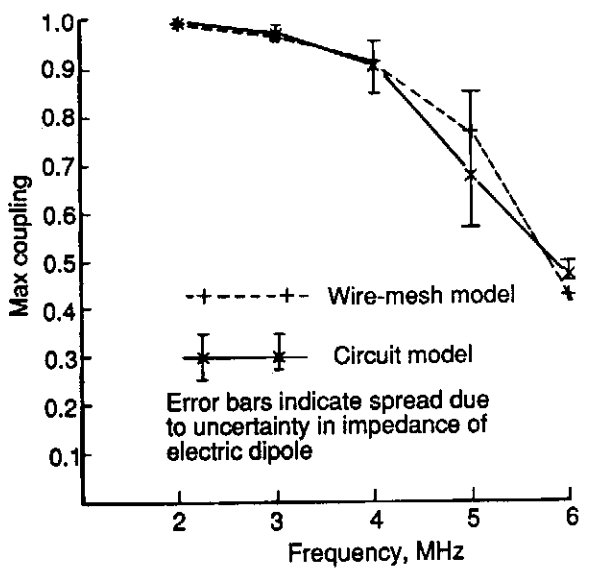


**Variation of maximum coupling between antennas versus frequency for wire-mesh and circuit models**

**Fig 6**

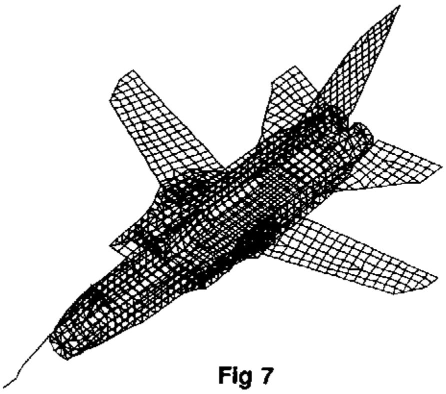

Fig 7

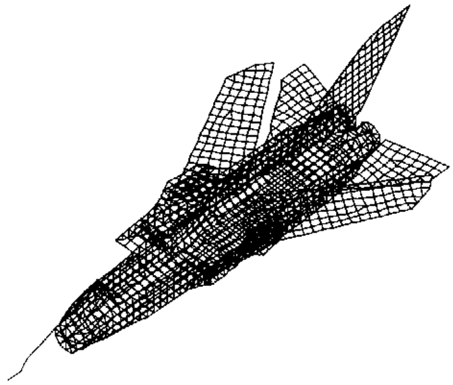

Fig 8

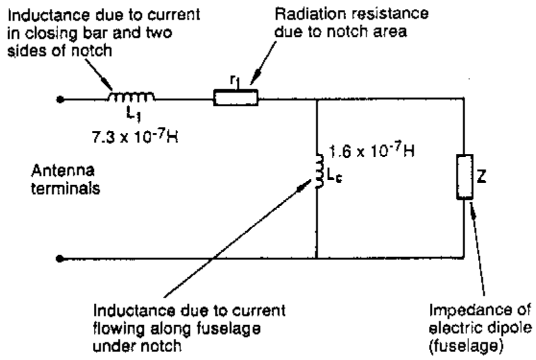


Approximate equivalent circuit of notch antenna and fuselage

Fig 9

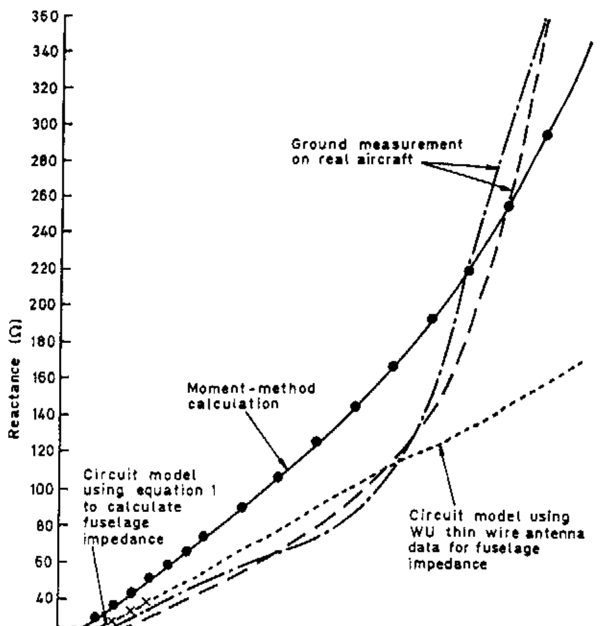


Terminal reactance-frequency (wings forward)

Fig 10

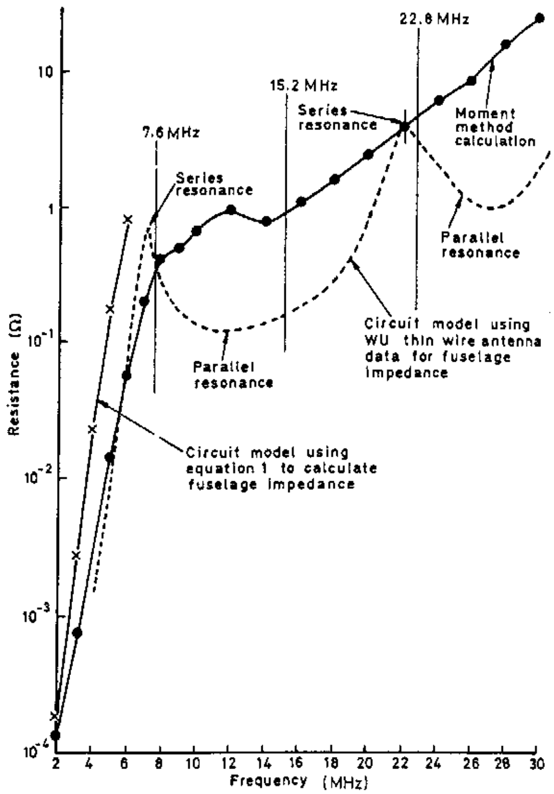


Radiation resistance (wings forward)

Fig 11

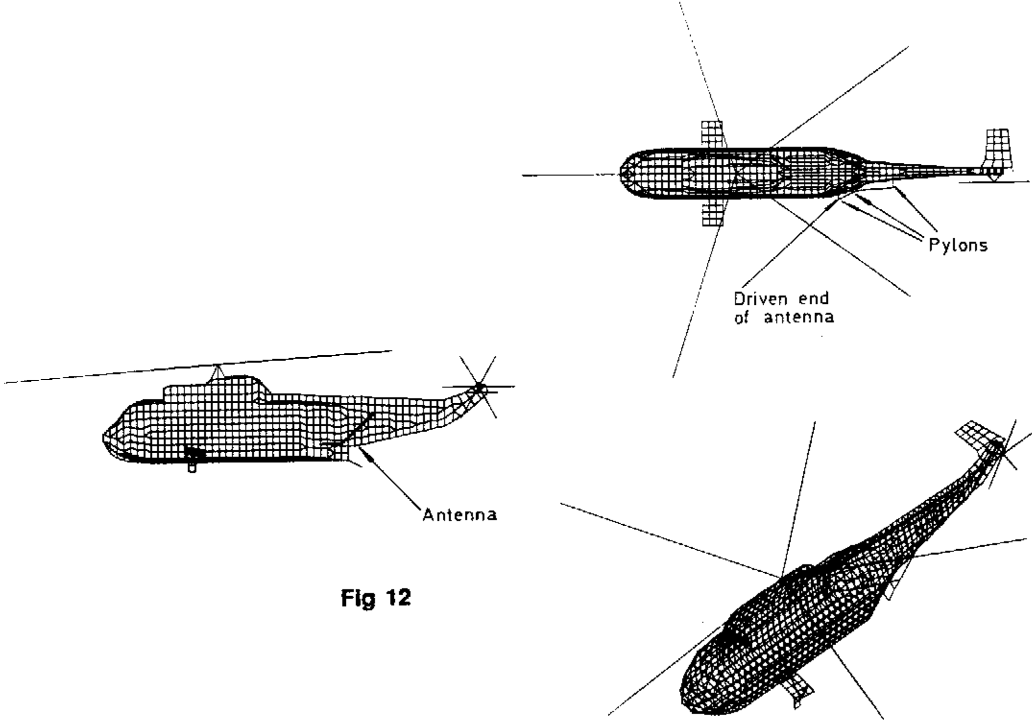


**Fig 12**

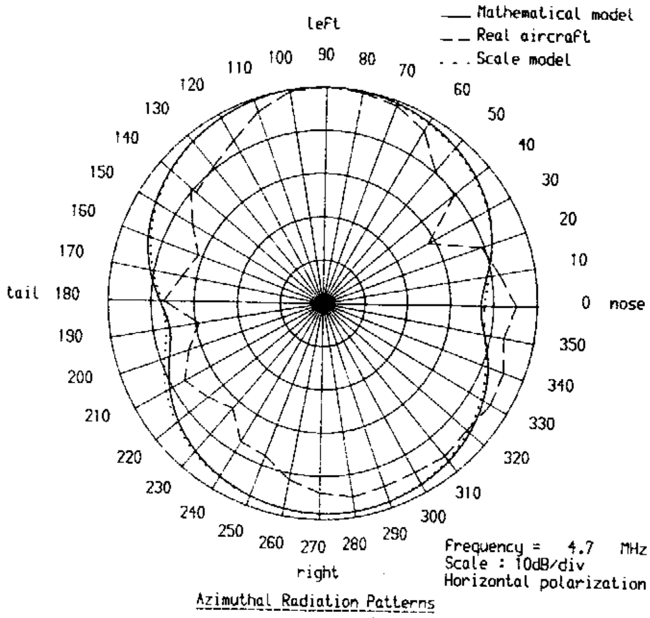


**Fig 13**

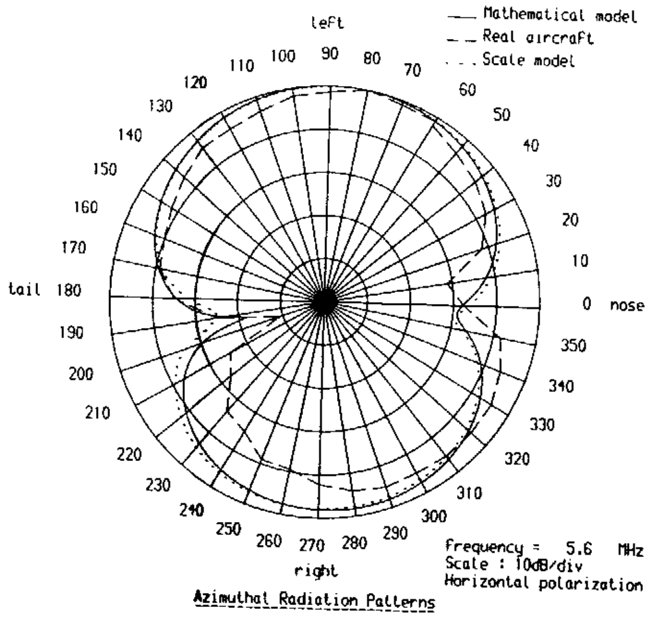


**Fig 14**

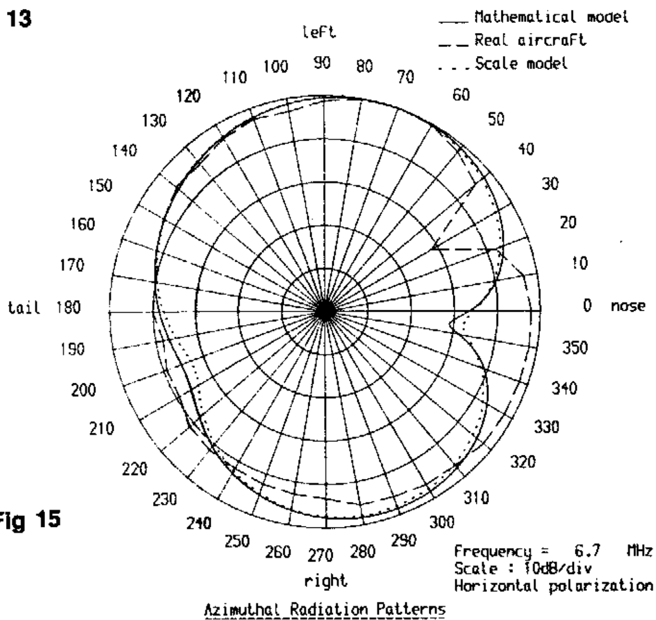


**Fig 15**